

## Experiments on Ekman layer instability

By P. R. TATRO AND E. L. MOLLO-CHRISTENSEN

Massachusetts Institute of Technology Department of Meteorology

(Received 5 July 1966)

Laboratory measurements were made of the instabilities of the Ekman layer using hot wire anemometers. The apparatus consisted of two parallel circular rotating plates forming a spool; the air was admitted through screens at the outer edge and removed through a screen cage at the hub. In the Ekman layers formed on the inner surfaces of the plates, measurements were made of the mean velocities as functions of  $r$  and  $a$ ; the velocity fluctuations were also measured.

It appears that the instability labelled type II by Faller always occurs first, and at zero Rossby number the critical Reynolds number is  $56 \pm 2$ . This instability originates in the boundary layer, but at slightly higher Reynolds number the fluctuations persist far into the geostrophic region, probably as inertial waves excited by the boundary-layer fluctuations.

At higher Reynolds number another instability appears of shorter wavelength and slower speed. This instability is confined to the boundary layer and is apparently the type I reported by Faller.

The phase speeds, frequencies, and wave-front orientations of both type instabilities have been measured.

---

### Review of previous work

During the drift of the 'Fram' across the polar sea (1893–96), Fridtjof Nansen observed that the direction of drift of the surface ice was 20–40 degrees to the right of the wind, and attributed this phenomenon to the effect of the earth's rotation. Nansen further reasoned that the direction of motion of each water layer must be to the right of the layer above it since it is affected by the overlying layer much as the surface layer is affected by the wind (Sverdrup *et al.* 1942).

At Nansen's suggestion, Ekman (1905) analysed this problem, and investigated the flow resulting from a balance of pressure gradient, Coriolis, and frictional forces. Ekman considered the eddy viscosity,  $A$ , to be constant, and showed that the important boundary-layer velocities are confined to a layer of thickness  $\sqrt{(A/\rho f)}$ , which he called the 'depth of frictional resistance'. Within the boundary layer, the velocity is represented by a vector which changes in length exponentially with depth, and angle linearly with depth. This is the familiar *Ekman Spiral*. Although Ekman considered an eddy viscosity, the analysis is applicable to laminar flows if the constant eddy viscosity  $A$  is replaced by a constant dynamic viscosity  $\mu$ . The Ekman solution for the components of a bottom boundary current under a velocity  $V$  in the  $x$  direction which is independent of depth is given by

$$\begin{aligned}V_x &= V(1 - e^{-z/D} \cos z/D), \\V_y &= V e^{-z/D} \sin z/D.\end{aligned}$$

Because of the similarity of the boundary-layer profiles in Ekman flow and the flow over a rotating disk in a fluid at rest (Schlichting 1960), it is interesting to consider the results of some early instability experiments with rotating disks in free air. Theodorsen & Regier (1947) made measurements with a fixed hot wire anemometer over a disk rotating in free air, in which they found a disturbance occurred at a transition Reynolds number of 1440, with the following definitions

$$Re_{\delta} = (\Omega r) \delta / \nu, \quad \delta = 2.58(\nu / \Omega)^{\frac{1}{2}}.$$

This corresponds to a Reynolds number of 560, when  $Re$  is defined as

$$Re = (\Omega r) / (\nu \Omega)^{\frac{1}{2}}.$$

Smith (1947) used a hot wire probe adjacent to a vertical rotating disk in air, and found sinusoidal disturbances to occur at

$$620 < Re_{\delta^*} < 760,$$

where

$$\delta^* = 1.37(\nu / \Omega)^{\frac{1}{2}}.$$

Eliminating the 1.37 factor, this corresponds to a Reynolds number range of

$$450 < Re < 555.$$

Smith, using a double wire probe, determined the phase velocity to be  $C = 0.2$  ( $r\Omega$ ), and the angle of orientation to be 14 degrees with respect to the tangential direction.

Gregory, Stuart & Walker (1955) used the china clay technique to determine the presence of instability on a rotating disk in free air. This technique is limited in that it is capable of demonstrating the presence only of stationary modes of disturbance. They found that an instability occurred at  $Re = 1.8 \times 10^5$ , with the Reynolds number defined as

$$Re = (\Omega r) r / \nu.$$

This reduces to a critical Reynolds number of 435 when the second  $r$  is replaced by the Ekman depth  $D$  in the computation of  $Re$ .

The direction of propagation of the waves as given by the china clay picture was 14 degrees from the radial direction, in good agreement with Smith's work and the theoretical calculations of Stuart in the same paper. Stuart's analysis indicated the instability to be in the form of a series of horizontal roll vortices with spacing related to the boundary-layer depth, an hypothesis which was reasonably well confirmed by the experimental work. Stuart concluded that the curvature terms had little influence on this inviscid instability.

Stern (1960) considered the theoretical problem of a fluid of relatively shallow depth in a rotating annulus, with fluid being forced in at the outer rim and withdrawn at the inner rim. This establishes a geostrophic azimuthal velocity over an inflowing viscous boundary layer. Stern theoretically established the possibility of the existence, at large Taylor numbers, of an instability which draws its energy from the ageostrophic perturbation component of the mean flow. He referred to this as a 'body-boundary' mode, and suggested that for Taylor numbers as large

as  $2.5 \times 10^3$  the flow should be unstable at Reynolds numbers below 80, and that the preferred mode of disturbance should have a radial wavelength given by

$$\lambda_r = (2\pi/m)Ta^{\frac{1}{2}}D,$$

where  $Ta$  is the Taylor number

$$Ta = \Omega H^2/\nu,$$

$H$  is the total fluid depth, and  $m$  is a constant of order unity.

Arons, Ingersoll & Green (1961) conducted a series of experiments in which they supplied water to the centre of a rotating tank partially filled with water, and allowed the surface to rise with time. They observed a highly organized pattern of instability in the form of concentric cylindrical sheets of water which rose as sharply defined jets through the entire depth of the fluid. This instability was confined to the narrow Reynolds number range

$$1.6 < Re = VD/\nu < 3.6$$

and had a wavelength given by  $\lambda = 2.0Ta^{\frac{1}{2}}D$ .

Faller (1963) conducted both a theoretical and an experimental study of Ekman layer instability in which he considered a rotating tank partially filled with fluid having a distributed source around the outer rim and a concentric sink at the centre. His analysis utilized an expansion in Rossby number of the non-dimensionalized dependent variables of the Navier–Stokes equations to form an ordered set of equations which could be solved subject to the appropriate boundary conditions. He found the radial component of the interior flow to be zero to the second order tangential velocity to be given by

$$V(2) = 1 - \frac{3}{10}R_0 + \frac{233}{600}R_0^2. \quad (1)$$

For his experimental work, Faller used a rotating tank four metres in diameter with a pumping system to withdraw water from the centre and distribute it uniformly around the outside. The boundary-layer circulation was observed by the introduction of potassium permanganate dye crystals near the outer rim, which tended to form streaklines as the fluid flowed past. Spiral bands of dye which formed were interpreted as regions where the layer of dyed fluid became deeper or shallower due to the superposition of unstable perturbations on the basic boundary-layer flow. Photographs of the bands were measured to give a critical radius at which the bands were first observed, their orientation, and their spacing.

Faller used the zero-order solution for the geostrophic velocity

$$V_\theta = S/\pi r D, \quad (2)$$

where  $S$  is the mass flow rate, in the definitions of Reynolds number and Rossby number

$$Re = S/\pi r \nu, \quad R_0 = S/2\pi r^2 \Omega D, \quad (3)$$

so that both parameters could be expressed in terms of only the two independent parameters,  $S$  and  $\Omega$ . The critical Reynolds number, in the limit of zero Rossby number, was found to be  $Re = 125 \pm 5$ . The wavelength, non-dimensionalized by the Ekman depth, varied from  $\lambda/D = 9.6$  to  $\lambda/D = 12.7$  with an average of 10.9.

The average angle from the tangential direction was found to be  $\epsilon = 14.5$  degrees to the left, with a standard deviation of 2.0 degrees. Motion pictures of the bands showed that in all cases they moved radially inward.

Barcilon (1965), in a theoretical paper, obtained analytic solutions of the perturbation equations using an Ekman mean velocity profile. He did not, however, arrive at a value for a critical Reynolds number since his method of solution was not accurate at the relatively small Reynolds numbers where instability has been observed.

Lilly (1966) and Faller & Kaylor (1966) at about the same time, presented numerical solutions to the Ekman layer problem. Lilly used a perturbation analysis and numerically solved both the complete set of equations and the Orr-Sommerfeld equation (OSE). Both solutions exhibited instability, with a minimum Reynolds number of 55 for the complete set and 85 for the OSE. Stationary waves were found to be unstable above  $Re = 115$ . Lilly suggested that the substantially lower critical Reynolds number for the complete set indicated the existence of a separate instability mechanism, associated with the Coriolis terms, and verified this by means of a simplified analytic solution. He designated this as a 'parallel instability', and noted that it was of the viscous type since it vanished at high Reynolds numbers. The numerical solution indicated that the viscous instability should be oriented at small or negative (to the right) angles with respect to the tangential flow.

Faller & Kaylor obtained numerical solutions to the time dependent non-linear equations of motion starting with a perturbation on the finite difference equivalent of a laminar Ekman solution. Their results confirmed the presence of two distinct modes of instability; one with  $\lambda = 11D$  and  $\epsilon = 12$  degrees, and a longer faster wave at negative  $\epsilon$  with a critical Reynolds number in the range  $50 < Re < 70$ .

In a recent experimental paper, Faller & Kaylor (1965) have reported the observation of the viscous instability occurring at lower Reynolds number, which they have designated type II. The apparatus used was essentially the same as was used earlier by Faller in his studies of the inviscid instability waves (type I). The type II waves were found to occur sporadically, move rapidly, have a wavelength of 22 to 33 times the Ekman depth, and to be oriented at an angle varying from 5 degrees to the left (+ 5 degrees) to 20 degrees to the right (- 20 degrees) of the tangential direction. These waves occurred at a minimum Reynolds number of  $Re = 70$ . It was observed that when the type II vortices attained finite amplitude before the type I were established, the combined circulation became unstable to a small scale mode, which then interacted with the previously established flow to produce an abrupt transition to turbulence.

### **Description of experiment**

Ekman boundary layers were generated by the removal of air from the centre of a rotating tank having the general shape of a flat spool with large flanges. Air was admitted at the outer edge after passing through silk screens which brought it up to solid body rotation.

Measurements were made of the mean velocity field between the plates at several radial positions; the onset of boundary-layer instability was observed as well as its further development, and the waves were measured. Hot wire anemometers were used for all measurements, and hot wire outputs were recorded as a function of position using an  $X$ - $Y$  recorder.

### Experimental equipment

The rotating tank consisted of two 36 in. diameter circular disks of 0.5 in. Plexiglas, held 3.00 in. apart by a hollow core at the centre and six spacers around the rim (figure 1). The main hollow shaft runs in two bearings, is driven by the belt from a variable speed hydraulic drive, and is connected through a rotating seal and a flowmeter to a variable speed vacuum cleaner.

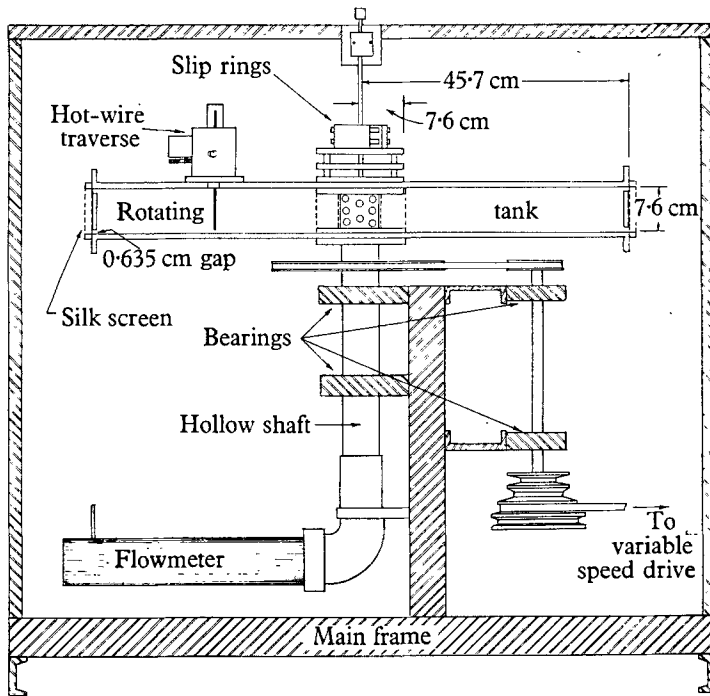


FIGURE 1. Diagram of apparatus.

Covering the space between the two outer rims are two 50-mesh silk screens spaced 0.5 in. apart. A Plexiglas baffle between the disks allows air to enter the tank only through 0.62 cm slots adjacent to the disks. Another silk screen was placed at a 3 in. radius around the central perforated hub. The entire system is supported by a steel frame which rests on rubber pads and can be levelled by screw adjustment.

The upper disk has five access holes,  $\frac{3}{4}$  in. diameter, at radii of 6, 8, 10, 12 and 14 in., to allow the insertion of hot wire assemblies. A slip ring assembly, consisting of nine silver rings with two silver-graphite brushes in each ring, is mounted on the top disk. As a matter of routing, two rings were used for each hot wire lead.

The traverse of the hot wire probe is motor driven, and connected to two precision potentiometers so that hot wire height and angle can be read as voltages. Hot wire signals were monitored on an oscilloscope, and recorded on an  $X-Y$  or an  $X-t$  recorder.

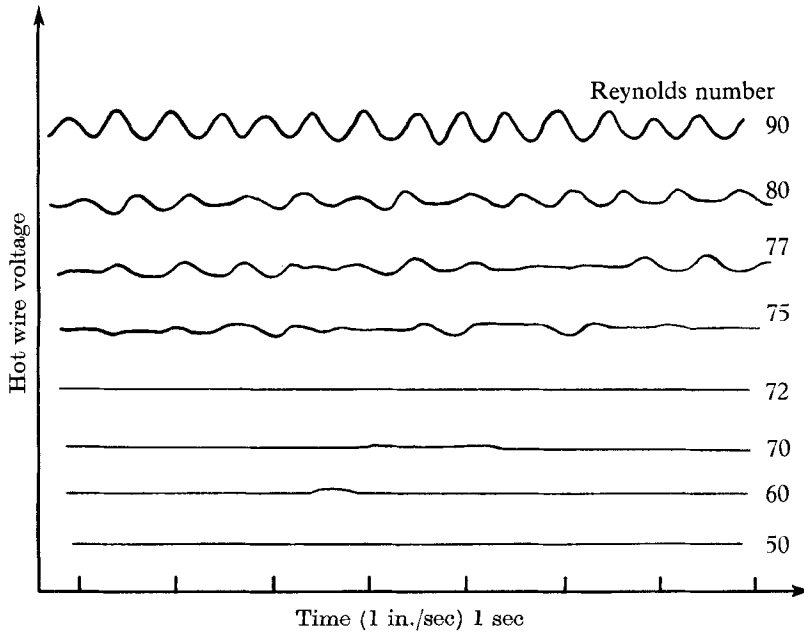


FIGURE 2. Traces of hot wire output voltage at constant  $\Omega$  at different Reynolds numbers, showing onset of instability. Vertical level offset changed for each trace.

### Experimental techniques

To detect the onset of instability, a hot wire was placed in the boundary layer approximately one Ekman depth from the boundary, and the  $X-Y$  recorder used to plot the hot wire voltage as a function of time. With the tank operating at a fixed rotational speed, the mass flow through the tank was incrementally increased, and the hot wire voltage recorded. For relatively low values of mass flow the recorder sweeps were essentially straight lines. As the mass flow is increased, however, the hot wire output voltage would begin to oscillate, and these oscillations plotted against time would be sinusoidal in appearance, as in figure 2. The lowest value of mass flow for which the oscillations could be observed was taken as the critical point.

At the critical point, the hot wire was rotated so as to have maximum sensitivity to the radial component of velocity, and then driven vertically to plot a vertical profile of radial velocity through the boundary layer. Since the theoretical Ekman radial velocity reaches a maximum at  $Z/D = \frac{1}{4}\pi$ , the measured boundary-layer thickness  $\delta$  was computed by measuring the  $Z$  co-ordinate of the maximum in the radial velocity profile, and taking  $\delta = 4Z/\pi$ .

At the same critical point, the geostrophic velocity well above the boundary layer was measured by means of a calibrated hot wire anemometer.

The hot wire signal, as monitored on an oscilloscope or recorder, is quite regular in appearance with increased mass flow from the critical point up to a second well-defined point. At this point, the character of the wave changes markedly and quickly. Figure 3*a* shows the wave-form just below this point, and figure 3*b* shows its appearance at this point. It appears that a different instability mechanism has occurred.

By utilizing a hot wire probe having two sensing wires and making phase comparisons of the signals, it is possible to determine the wave-front orientation and the phase speed. An oscilloscope was used with Lissajous figures to determine the in-phase point, and a double channel chart recorder to determine phase differences.

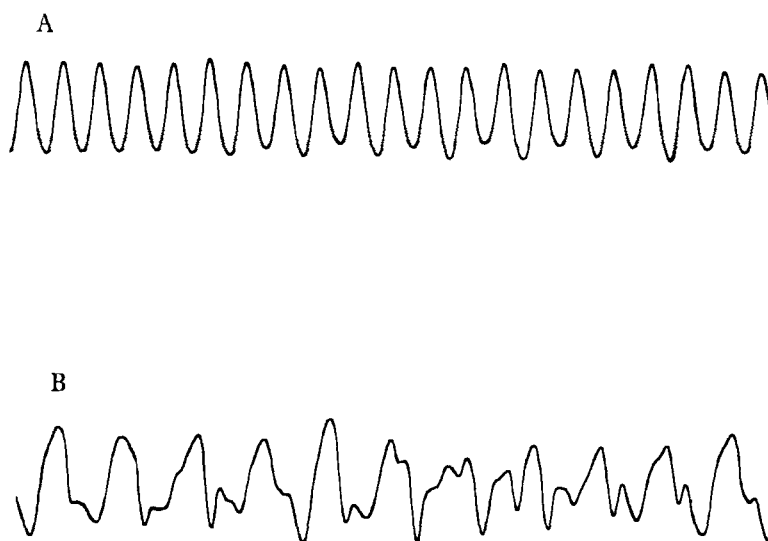


FIGURE 3. Wave-forms of hot wire output showing development near  $Re = 125$ . A, Wave-form at Reynolds number 126; B, wave-form at Reynolds number 130.

## Results

The geostrophic velocity  $V_g$  was measured as a function of the radial position for several combinations of parameters. Figure 4 is a typical  $V_g(r)$  result. The measured velocities were in all cases less than the theoretical values based on mass flow, with the measured values approaching the theoretical as the Rossby number approached zero.

Profiles of the tangential velocity  $V$  and the radial velocity  $V_r$  made through the boundary layer below the first critical point were in good agreement with Ekman theory. Figure 5 shows sample profiles. Above the critical point, the instability shows up in the  $V(z)$  and  $V_r(z)$  profiles, but is confined to the boundary layer, figure 6.

For each combination of mass flow and rotation at which a critical point was determined, a Reynolds number and Rossby number based on local measured values of the parameters were computed

$$Re = V_g \delta / \nu, \quad R_0 = V_g / 2\Omega r.$$

Figure 7 shows a plot of the critical Reynolds number versus Rossby number. The instability identified by Faller & Kaylor 1965 as type II always appeared first. A least-squares linear regression for the type II was found to be

$$Re_{IIc} = 56.3 + 116.8R_0.$$

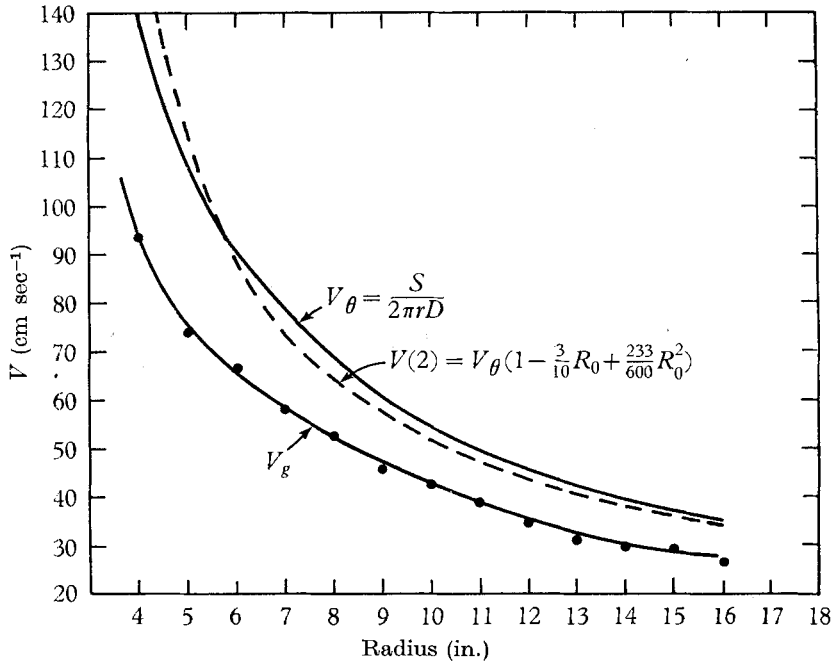


FIGURE 4. Azimuthal velocity vs. radius.  $V_g$  measured,  $V_\theta$  theoretical based on ideal Ekman layer transport and  $V(2)$  given by equation (1).

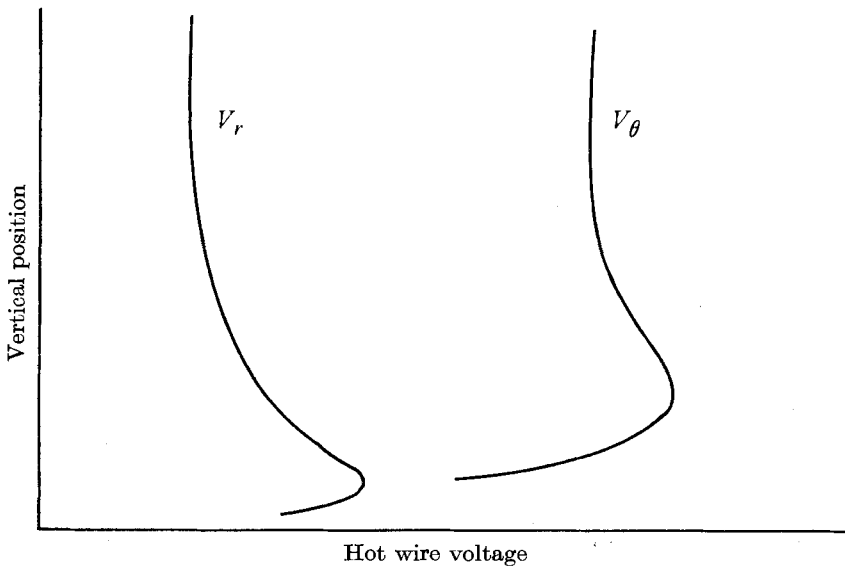


FIGURE 5. Hot wire voltage vs.  $Z$  for wire aligned with rank radius ( $V_\theta$ ) and wire normal to radius ( $V_r$ ), below critical  $Re$ .

The measurements of geostrophic velocity are considered to have an accuracy of  $\pm 0.5 \text{ cm sec}^{-1}$ , and the boundary-layer thicknesses are considered accurate to within  $\pm 0.004 \text{ cm}$ , hence the critical Reynolds number for type II waves is taken to be

$$Re_{IIc} = 56.3 \pm 2.0.$$

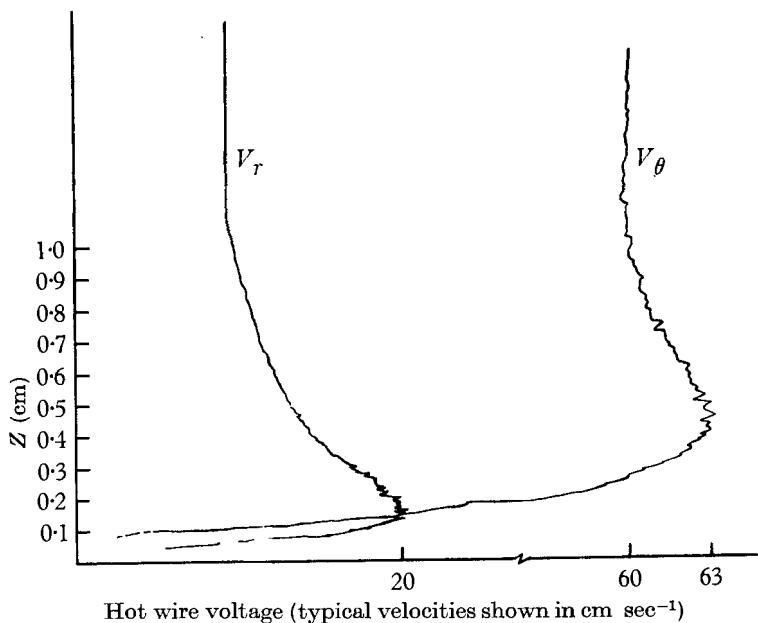


FIGURE 6. Hot wire voltage vs.  $Z$  just above critical  $Re$ .

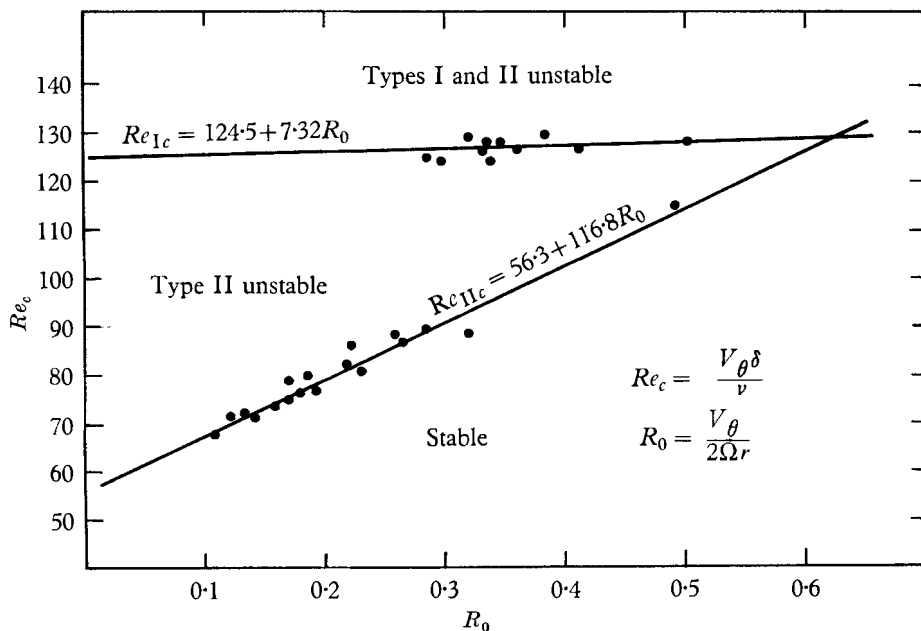


FIGURE 7. Critical Reynolds number vs. Rossby number for types I and II instabilities.

The marked change in the instability, discussed earlier, was identified as the type I instability originally reported by Faller (1963). A linear regression for ten points for this instability yielded

$$Re_{Ic} = 124.5 + 7.32R_0$$

which was in such close agreement with earlier work that it was not felt necessary to make further measurements of the type I. The experimental accuracy in  $Re_{Ic}$  is estimated as 2%.

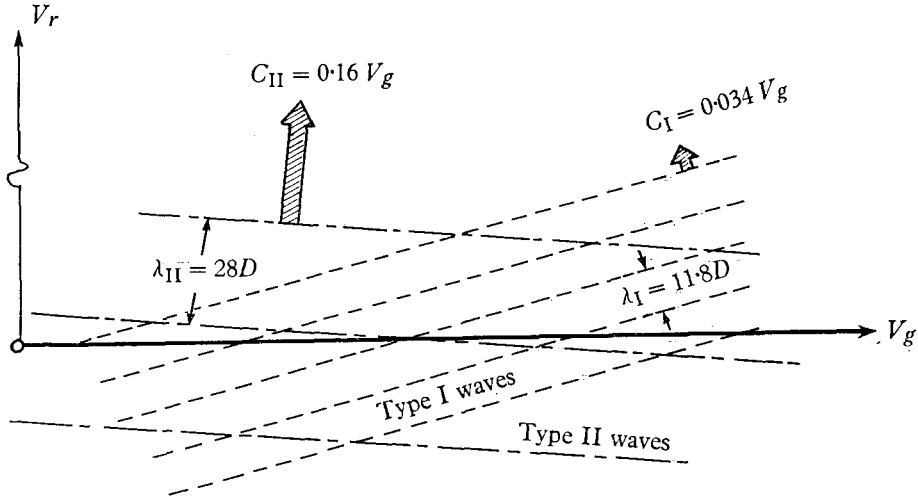


FIGURE 8. Diagram of measured wavelengths, phase velocities and wave-front orientations.

The wavelength and orientation of both types of waves were determined with a double wire probe, and the general arrangement of these results is shown in figure 8. The non-dimensional wavelength  $\lambda/D$  of the type II waves was found to vary from  $\lambda/D = 25.0$  to  $\lambda/D = 33.0$  with a mean of 27.8 and a standard deviation of 2.0. Considering the characteristic angle of the Ekman spiral with respect to the interior flow to be a positive angle, the orientation of the type II varied from 0 degrees to  $-8$  degrees. The phase velocity was approximately 16% of the geostrophic velocity and directed radially inward.

The type I waves were found to have a nearly constant angle of  $\epsilon = 14.6$  degrees with respect to the geostrophic flow with a standard deviation of 0.8 degrees. The non-dimensional wavelength was found to be  $\lambda/D = 11.8$ , and the radially inward phase velocity was 3.4% of the geostrophic velocity.

As has been shown, the type II instability originates in the boundary layer. As the Reynolds number is increased above the critical value, however, the oscillations do not remain confined to the boundary layer, but rather seem to propagate throughout the entire interior region. Figure 9 shows a vertical profile of the radial velocity component with these oscillations superimposed. They extend without noticeable attenuation of amplitude up through the geostrophic region.

### Discussion

All earlier attempts to measure or define an instability point in Ekman flow have depended on techniques which were responsive only to stationary or at best slowly moving waves. The fast response and high sensitivity of a hot wire anemo-

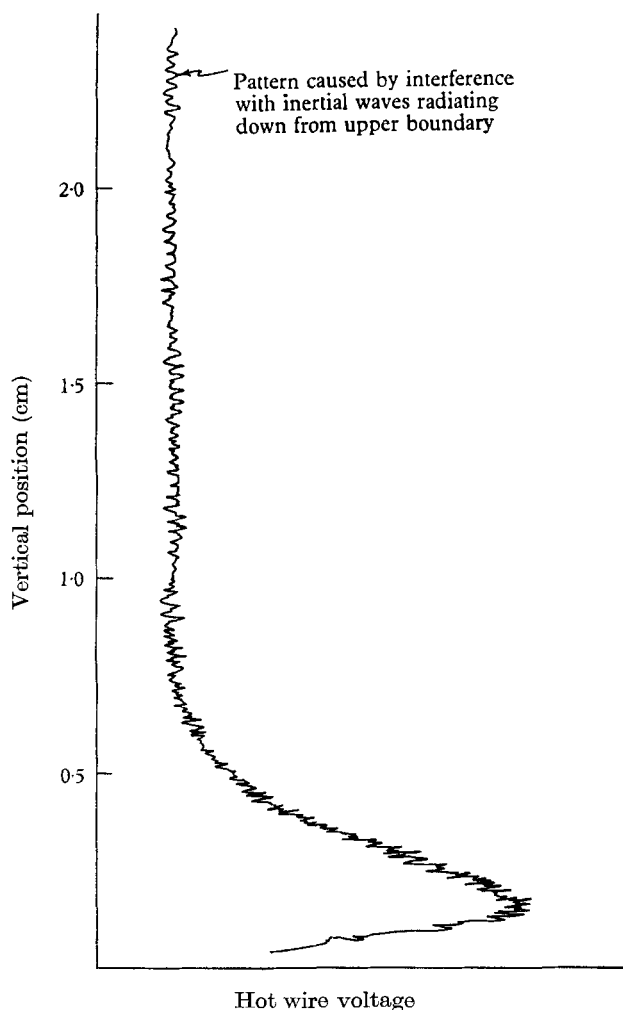


FIGURE 9. Hot wire voltage *vs.* height  $Z$  showing oscillations penetrating into geostrophic region. The wire was moved slowly in the  $Z$ -direction at constant speed, so that oscillations would be shown superimposed on mean velocity profile.

meter rotating with the system have made possible the detection of a faster, longer wave, and allowed the direct measurement of the pertinent local parameters.

The vertical profiles of the horizontal velocity components exhibit oscillations throughout the interior region. We infer that these are inertial waves from the

following arguments. Consider a time-dependent perturbation equation for the interior, which assumes small Rossby number

$$\frac{\partial \mathbf{v}}{\partial t} + 2\boldsymbol{\Omega} \times \mathbf{v} = -\nabla(p/\rho).$$

Operating on this equation with CURL to eliminate the pressure gradient term, and assuming a periodic solution of the form

$$\{u, v, w\} = \{\hat{u}, \hat{v}, \hat{w}\} \exp [i(kx + ly + mz - \omega t)]$$

yields three linear homogeneous equations in three unknowns. The requirement that the determinant of the matrix of coefficients vanish for the existence of a non-trivial solution yields

$$\left[ \frac{2\Omega im}{\omega} \right] \left[ \left( \frac{2\Omega im}{\omega} \right)^2 + (k^2 + l^2 + m^2) \right] = 0$$

which may be satisfied either by  $m \equiv 0$ , or by

$$m = \pm i \sqrt{\left( \frac{k^2 + l^2}{1 - (4\Omega^2/\omega^2)} \right)}.$$

Three possibilities now exist: (1)  $\omega < 2\Omega$ , the radical is imaginary and the wave has a vertical wave number; (2)  $\omega > 2\Omega$ , the radical is real and the wave has an exponential vertical decay; and (3)  $\omega = 2\Omega$ , in which case the radical becomes infinite and the choice  $m = 0$  must be taken.

The type II instability has been shown to originate in the boundary layer, and it generally occurs with  $\omega > 2\Omega$ . As the amplitude increases, however, an inertial response seems to be stimulated; the first subharmonic becomes dominant above the boundary layer such that  $\omega$  is less than  $2\Omega$  and the wave is found throughout the interior region.

The type I instability occurred initially in the boundary layer, and at its onset was confined to the boundary layer. Since the type II always occurred with the type I, and the first manifestations of turbulence were generally noticed at only slightly higher Reynolds number, the vertical development of the type I was not investigated further.

## Conclusions

Although it is apparent from the measured variation of the tangential velocity with  $r$  (figure 4) that the flow outside the boundary layer is not purely geostrophic, the results show that the instability depends upon local measured Reynolds number and Rossby number only (figure 7).

The occurrence of oscillations which might be inertial waves is interesting. Before one can be sure further measurements of phase surfaces and wavelengths will be necessary. If the observed fluctuations are indeed inertial waves, any theory to account for instabilities of the Ekman layer for which  $\omega < 2\Omega$  will have to include a radiation boundary condition at  $Z = \infty$ .

Further measurements will also be required before one can describe the details of the process of transition to turbulence in an Ekman layer. From preliminary

observations of transition, it is apparent that bursts of high frequency fluctuations do appear, as they do in a flat plate boundary layer, and that a low frequency periodic structure may persist to Reynolds numbers well above transition.

The type II instability always occurred first, and at a sufficiently low Reynolds number such that the atmosphere would be above critical Reynolds number at wind speeds as low as six knots. The inertial waves stimulated by the boundary-layer oscillations extended throughout the interior region of the rotating model, and in a geophysical situation could account for spatial periodicity in temperature or humidity measurements well above the atmospheric Ekman layer.

Lieutenant-Commander P. R. Tatro, U.S.N., was supported by the U.S. Navy during the work; the work was supported by NASA under Grant NsG-496.

## REFERENCES

- ARONS, A. B., INGERSOLL, A. P. & GREEN, T. 1961 Experimentally observed instability of a laminar Ekman flow in a rotating basin. *Tellus*, **13**, 31-39.
- BARCILON, V. 1965 Stability of a non-divergent Ekman layer. *Tellus*, **17**, 53-68.
- EKMAN, V. W. 1905 On the influence of the earth's rotation on ocean currents. *Arkiv. Mat. Astr. Fys.* Bd 2, no. 11, 53 pp.
- FALLER, A. J. 1963 An experimental study of the instability of the laminar Ekman boundary layer. *J. Fluid Mech.* **15**, 560-576.
- FALLER, A. J. & KAYLOR, R. E. 1965 Investigations of stability and transition in rotating boundary layers. Tech. Note BN-427, Institute for Fluid Dynamics and Applied Mathematics, University of Maryland.
- FALLER, A. J. & KAYLOR, R. E. 1966 A numerical study of the instability of the laminar Ekman boundary layer. *J. Atmos. Res.* **23**, 481-494.
- GREGORY, N., STUART, J. T. & WALKER, W. S. 1955 On the stability of three-dimensional boundary layers with application to the flow over a rotating disc. *Phil. Trans. A* **248**, 155-199.
- LILLY, D. K. 1966 On the instability of Ekman boundary flow. *J. Atmos. Res.* **23** (submitted for publication).
- SCHLICHTING, H. 1960 *Boundary Layer Theory*, 4th ed. McGraw-Hill.
- SMITH, N. H. 1947 Exploratory investigation of laminar boundary layer oscillations on a rotating disc. *NACA Tech. Note* 1227.
- STERN, M. E. 1960 Instability of Ekman flow at large Taylor number. *Tellus*, **12**, 399-417.
- SVERDRUP, H. U., JOHNSON, M. W. & FLEMING, R. H. 1942 *The Oceans*. Prentice-Hall.
- THEODORSEN, T. & REGIER, A. 1947 Experiments on drag of revolving discs, cylinders, and streamline rods at high speeds. *NACA Rep.* no. 793.